Musa paradisiaca extract as a corrosion inhibitor of steel. Role of KI as a synergistic additive

J.R. Torres-Hernandez,[1] E. Del Ángel-Meraz,[1]* F.E Corvo-Pérez,[2] M.G. Rivera-Ruedas,[1] M.A. Hernández-Rivera[1] and J. Barajas-Fernández

[1]Juarez Autonomous University of Tabasco, Postgraduate in Engineering Sciences, Carretera Cunduacan-Jalpa Km. 1, Col. La Esmeralda, c.p. 86690, Cunduacan, Tabasco, México

[2]Autonomous University of Campeche, Corrosion Research Center, Corrosion Research Center, Av. Agustin Melgar S/N, street 20 between and Juan the Barrera, Col Buenavista, c.p. 24039, Campeche, México

**E-mail: bellita.delangel@gmail.com*

Abstract

The synergistic effect of KI addition to the system *Musa paradisiaca* shell (ECMP–KI extract) with ethanol/water on SAE 1010 carbon steel in 1 M HCl solution was studied. *Musa paradisiaca* (ECMP extract), was obtained by Soxhlet extraction with ethanol/water and characterized by gas chromatography (GC-MS). The following main components were found: $C_{18}H_{36}O$ (octadecane), $C_{16}H_{32}O_2$ (palmitic acid) and C_6H_6O (phenol). The weight loss (WL) shows a maximum efficiency of 91% with ECMP extract and 93% with ECMP–KI extract. Electrochemical impedance (EIS) and potentiodynamic polarization (PDP) tests were performed at three immersion times: t_1: 1 h, t_2: 24 h, and t_3: 48 h. The obtained efficiencies by EIS with ECMP extract were in the range 75–93% and 80–94% for the system ECMP–KI. The addition of KI showed a slight increase in efficiency, but higher than under WL evaluation. Respecting PDP technique, it was possible to identify ECMP extract as a mixed type inhibitor for the three immersion times, obtaining efficiencies of 76–91% with ECMP extract and 78–93% for ECMP–KI extract. Data obtained from the EIS and PDP electrochemical techniques were fitted to Langmuir, Temkin and Freundlich adsorption isotherm models. It was observed that the Langmuir model showed the best fit for the ECMP extract and for ECMP–KI extract. Only a slight effect of KI as a synergistic additive was observed, possibly because the extract shows high inhibitory efficiency, and the surface was already saturated with the adsorbed natural inhibitor.

Received: July 31, 2023. Published: December 15, 2023 doi: 10.17675/2305-6894-2023-12-4-50

Keywords: *carbon steel, green inhibitor, Musa paradisiaca, synergistic additive.*

1. Introduction

Corrosion of steel and other metals commonly causes economic losses in the process industry due to equipment failures. Steel is the most commonly used material for the

construction of industrial plants and pipelines, due its mechanical properties, versatility and cost. The costs of corrosion represent between 2–4% of the gross national product [1–3].

To increase the service life of steel, it is necessary to mitigate corrosion. Many investigations are dedicated to protecting metals from corrosion. Different corrosion prevention methods are commonly applied, such as coatings, cathodic protection and inhibitors. The type of preventive method is selected according to the environment and the conditions to which the metal is exposed [4, 5]. In general, in the case of internal corrosion in pipes or storage tanks, organic and inorganic inhibitors are used. Inorganic or synthetic corrosion inhibitors are efficient, but they are expensive and can cause dangerous environmental effects due to their toxicity and negative effect to the environment [6, 7].

Organic inhibitors are currently more used. It is important to consider modifications made to ISO 14001 standard, where it is specified that corrosion inhibitors must not be "toxic to human life" and their composition must not contain heavy metals and must be environmentally friendly [8, 9].

Inhibitors obtained from plant extracts, known as "green inhibitors", promise to be an efficient and non-toxic alternative to corrosion inhibitors. These types of inhibitors contain different natural components that can have inhibitory effects [10, 11]. Products defined as "Green corrosion inhibitors", based on natural products such as fruits, plants, bark, seeds, and leaves have been investigated for its antioxidant properties and low cost for its preparation. They contain compounds that facilitate the exchange of electrostatic charges, creating an absorbed protective layer capable of minimizing the effect of corrosion [3, 12–14].

In small amounts, corrosion inhibitors can delay or slow down the rate of corrosion of fluid transport pipelines by affecting anodic and/or cathodic reactions. Molecules having inhibitor effect are characterized for containing elements such as N, S, P, and O, considered as heteroatoms. These elements cause changes in the electronic molecular density of the metal that facilitate its protonation in acid medium. If the metal surface is negatively charged, the adsorption of the molecule on the surface and the formation of a protective adsorbed layer on the metal of which the pipe or storage container is made. In the particular case of natural extracts, several molecules with quite similar characteristics that are adsorbed on the surface can cause the inhibitory effect [15–19].

The inhibition capacity of the aqueous extract of the *Musa paradisiaca* shell in HCl has been reported, using three types of shells: green, ripe and tall ripening. Green peel showed the better efficiency. Using electrochemical impedance (*IE*) technique, efficiencies in the range of 81 to 89±4.04% were determined and by using potentiodynamic polarization (PPD) technique, the efficiencies were in the range 82 to 90±4.04%, with this technique the extract was classified as an anodic inhibitor. It was proposed that the inhibition potential is due to the content of gallocatechin ($C_{15}H_{14}O_7$) and catechin ($C_{15}H_{14}O_6$) molecules [20].

The efficiency of *Musa paradisiaca* leaf aqueous extract was determined at temperatures of 298, 308, 318 and 328 K, on steel immersed in H_2SO_4 at concentration of

3 g/L was in the range from 81.9 to 57.8±7.05 %, showing that an increase in temperature causes a decrease in efficiency. The inhibition mechanism is of a mixed type [21]. The extract of the *Musa paradisiaca* leaf in water collected in a marine environment was also evaluated using the potentiodynamic polarization measurements, they tested 0–1000 ppm concentrations of the extract and found an efficiency in the range 66.19% to 86.51% at 30 min immersion time, they classified it as a mixed type inhibitor [22]. *Musa paradisiaca* husk extract powder was tested in HCl. Maximum efficiency of 87% was determined on steel at concentration 500 ppm [23].

The evaluation of *Hymenaea stigonocarpa* fruit peel extract as steel corrosion inhibitor in sulfuric acid has been reported. By using potentiodynamic polarization analysis this extract was classified as mixed type inhibitor with maximum efficiency of 87% [12]. The evaluation of pectin in H_2SO_4 showed an efficiency of 76.43% and mixed type inhibitor behavior [24]. *Murraya koenigii Linn* in hydrochloric acid and evaluated by EIS showed an efficiency of 80.65% on steel, while through PPD showed efficiency of 85.71% and mixed type behavior [25]. In other investigations the extract of white tea in hydrochloric acid achieves efficiencies of 96.0% [26]. The behavior of amino acid cysteine in hydrochloric acid showed an efficiency of 90% with the PDP technique. It behaves as a mixed type inhibitor [27]. The peel of garlic (*Allium sativum L*.) and cocoa husk (*Theobroma L*.) showed efficiencies of 90.7% and 89% respectively, being both mixed type inhibitor [28].

The behavior of halide ions as synergic additives on organic inhibitors in acids has been studied. The increase in inhibition efficiency has been verified in many cases. The synergy is caused by the interaction of the inhibitor with the halide ion on the metal surface with a frequently significant increase in the inhibitory efficiency [29, 30]. The inhibitor efficiency can be increased by addition of a synergic additive, and at the same time, it is possible to minimize the required amount of the inhibitor. Usually, it is possible to increase the inhibition efficiency in an acid medium by adding halide salts such as potassium iodide (KI), potassium chloride (KCl) or potassium bromide (KBr) [31, 32].

However, it was observed that, according to the size and polarization, iodide ions (I^-) are the ones showing a greater synergistic effect, followed by Br^- and Cl^-. In the case of organic inhibitors, there is the possibility to increase inhibition efficiency by adding KI, which is adsorbed on the metal surface and thus can reduce static charges [33–34].

In the present paper, the ethanol/water extract of the green peel of *Musa paradisiaca* (ECMP) was evaluated as steel corrosion inhibitor in acid media at concentrations 200 ppm to 1000 ppm with and without the addition of KI (ECMP–KI). The addition of KI to ECMP extract has not been previously reported in the literature. The objective of this research is to determine whether KI can improve the inhibitor efficiency of the *Musa paradisiaca* extract as a corrosion inhibitor. The development of the *Musa paradisiaca* extract as a green inhibitor could support the economy of the farmers [20] in the Tabasco region, being one of the states with the highest plantain production in southeastern Mexico of approximately 2 million tons per year [35, 36].

2. Experimental Part

2.1. ECMP Extract

Figure 1 shows the methodology used to obtain the ECMP extract. It is divided into two stages:

1) *Musa paradisiaca* shells are abundantly washed with tap water, cutting them in pieces of 1×4 cm size and drying them in a stove at temperature 343 K for four hours. After removing from the stove, they were shredded in a mortar.
2) Sample already dried and shredded goes through the extraction process, using the Soxhlet equipment that contains ethanol and deionized water (4:1) as solvent. To obtain the ECMP–KI extract, a KI solution is added to the extract.

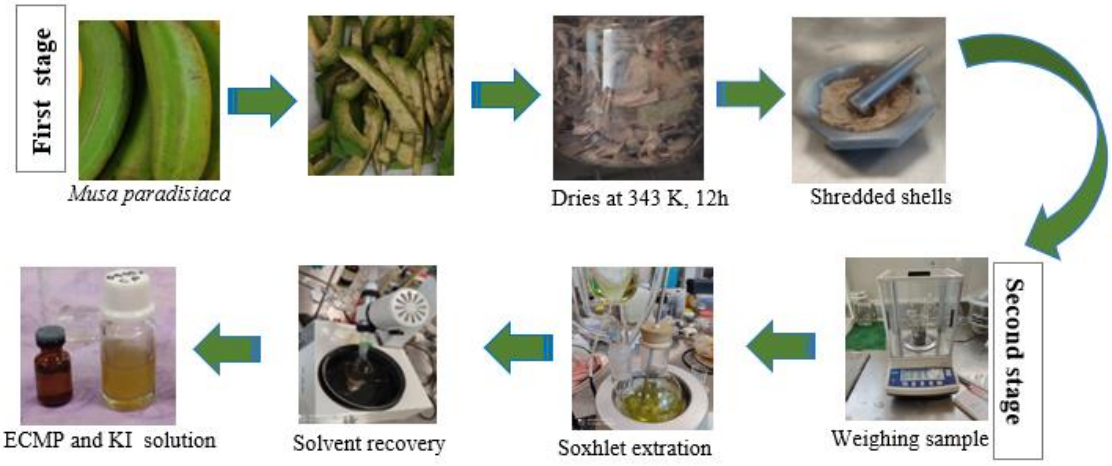

Figure 1. Scheme of Soxhlet extraction process from *Musa paradisiaca* green shells. Last image: ECMP extract and KI 100 ppm solution.

2.1.1. GC-MS Analysis

The ECMP extract was analyzed by gas chromatography and mass spectrometry (GC-MS) using a Shimadzu brand instrument, model GCMS-QP2010 ultra, with a helium gas flow 1.5 mL/min, and a capillary column (30 m×0.25 mm i.d., 0.25 µm film thickness, 5% the phenyl and 95% the dimethylpolysiloxane).

2.2. Weight Loss (WL)

Metal samples (3 cm×3 cm×1 cm), previously polished and cleaned with acetone, were immersed in 100 ml of 1 M HCl solution. The first stage of tests was carried out under the addition of ECMP extract in concentrations of 0, 200, 400, 600, 800 and 1000 ppm to test its corrosion inhibitor efficiency. The second stage was carried out adding ECMP extract as corrosion inhibitor and KI as synergic additive (ECMP–KI). The immersion time was six

days at room temperature. After the immersion time, the samples were washed with deionized water, soapy water and finally acetone and placed in a desiccator for one hour. The weight difference was used to calculate the inhibition efficiency using Equations 1 and 2 [27, 28].

$$W_{\text{corr}} = \frac{\Delta m}{St} \tag{1}$$

$$\eta = \left(W_{\text{corr}} - W'_{\text{corr}}\right) \Big/ W_{\text{corr}} \cdot 100 \tag{2}$$

where, $\Delta m = m_1 - m_2$ (mg); m_1: initial mass; m_2: final mass; S: sample area (cm^2), t: immersion time (min); W_{corr}: corrosion rate without inhibitor; W'_{corr}: corrosion rate in the presence of inhibitor, η = inhibitor efficiency (%).

2.3. Electrochemical Impedance Spectroscopy (EIS)

The EIS tests were carried out using the 128-PGSTAT potentiostat-galvanostat instrument. A three-electrode cell was used, consisting of a calomel reference electrode (SCE), a platinum counter electrode (CE), and a working electrode (WE). A solution of HCl (1 M) was used as electrolyte, at room temperature (298 K), during immersion times of 1 h (t_1), 24 h (t_2) and 48 h (t_3). ECMP extract was added in the range of concentrations from 200 to 1000 ppm.

EIS tests were performed in the frequency range 10000 to 0.01 Hz and using a signal of 10 mV with 10 points per decade. The Z_{sim} software was used to fit data from EIS spectra, each experiment was repeated three times. Efficiency was calculated according to Equation 3 [26].

$$\eta = \frac{R_{\text{ct}} - R'_{\text{ct}}}{R_{\text{ct}}} \cdot 100 \tag{3}$$

where, η: inhibitor efficiency (%); R_{ct}: charge transfer resistance determined in the presence of inhibitor; R'_{ct}: charge transfer resistance of steel determined in blank solution (without addition of inhibitor).

Double layer capacitance was calculated according to Equation 4 [30]:

$$C_{\text{dl}} = 1/(2\pi \cdot f_{\text{max}} \cdot R_{\text{ct}}) \tag{4}$$

where, f_{max}: maximum frequency at the vertex of the Nyquist diagram.

2.3.1. EIS tests determined in the presence of KI as a synergic additive

To evaluate the effect of the addition of iodide ions (I^-) to the system ECMP–SAE 1010 steel–1 M HCl, an aqueous solution of KI was added to the system. Subsequently, electrochemical impedance spectroscopy measurements were carried out in a concentration range from 200 to 1000 ppm of ECMP extract with 100 ppm of KI solution at three immersion times: 1 h, 24 h and 48 h.

Synergistic parameters were calculated to describe the inhibition behavior of the ECMP–KI extract combination. Equations 5 and 6 were used [32]:

$$S_1 = (1-\theta_{1+2})/(1-\theta'_{1+2}) \quad (5)$$

$$\theta = (\theta_1+\theta_2)-(\theta_1\cdot\theta_2) \quad (6)$$

where, S_1: synergy index; θ_1: surface coverage corresponding to KI; θ_2: surface coverage corresponding to ECMP extract; θ'_{1+2}: surface coverage ECMP+KI extract.

If $S_1 = 1$, there is no interaction between ECMP extract and KI. If $S_1 > 1$, there is a synergic effect between the two surface active ingredients. If $S_1 < 1$, there is an antagonistic effect between the two surface active ingredients.

2.4. Potentiodynamic Polarization (PDP)

PDP curves were performed in the range –0.250 V to +0.250 V at a sweep rate of 1 mV/s with respect to open circuit potential (OCP). Inhibitory efficiency was calculated according to Equation 7 [34]:

$$\eta = \left(I^0_{corr} - I^i_{corr}\right)/I^0_{corr}\cdot 100 \quad (7)$$

where, I^0_{corr} = current density of steel in blank solution (no inhibitor), I^i_{corr} = current density of steel in the presence of inhibitor, η = efficiency (%).

The effect of the addition of iodide ions in a concentration of 100 ppm (I^-) to the system ECMP extract–steel–HCl using polarization curves was evaluated in the concentration range 200–1000 ppm ECMP extract at three immersion times: 1, 24, and 48 h.

2.5. Surface characterization

The steel surface was characterized using the JEOL JSM-6010LA scanning electron microscope at an accelerating voltage of 20 kV, under high vacuum conditions. An energy dispersive spectrometer (EDS) coupled to the SEM was used to perform the semi-quantitative analysis and determine the distribution of elements on the steel surface. SAE 1010 steel plates were analyzed under four conditions:

- Surface after cleaning and polished with 600 to 1200 grit SiC sandpaper.
- Surface exposed to the corrosive solution without addition of inhibitor.
- Surface exposed to corrosive solution with the addition of 1000 ppm of ECMP extract (maximum inhibitor efficiency).
- Surface exposed to corrosive solution with the addition of 1000 ppm of ECMP extract and 100 ppm KI.

2.6. Adsorption isotherms

Inhibitory efficiencies (η) determined by weight loss (WL), potentiodynamic polarization (PDP) and electrochemical impedance spectroscopy (EIS) at different concentrations of

ECMP extract and ECMP–KI extract, at different immersion times, were fitted to the Freundlich, Langmuir and Temkin adsorption isotherm models, (Equations 8–10) [27].

$$\text{Langmuir adsorption isotherm } C_{\text{inh}}/\theta = 1/K_{\text{ads}} + C_{\text{inh}} \quad (8)$$

$$\text{Temkin adsorption isotherm } \log(C_{\text{inh}}/\theta) = \log K_{\text{ads}} - g\theta \quad (9)$$

$$\text{Freundlich adsorption isotherm } \log\left[\theta/(1-\theta)C_{\text{inh}}\right] = \log K_{\text{ads}} + g\theta \quad (10)$$

where, C_{inh}: ECMP extract concentration or ECMP–KI extract (ppm); θ: coverage area; K_{ads}: adsorption–desorption equilibrium, constant, and g: adsorbate interaction parameter.

The coverage area (θ) is directly proportional to η. The equilibrium constant (K_{ads}) was calculated using Equation 11 corresponding to Langmuir equation [34], where y is the slope.

$$K_{\text{ads}} = 1/y \quad (11)$$

where, y = slope.

3. Results and Discussion

3.1. GC-MS analysis of the extract

Table 1 shows ECMP extract composition determined by GC-MS analysis. Octadecan ($C_{18}H_{36}O$), a long-chain aldehyde, showed the highest percentage of area, followed by phenol (C_6H_6O), propane-1,2,3-triol ($C_3H_8O_3$), and palmitic acid ($C_{16}H_{32}O_2$).

These four molecules contain oxygen atoms causing differences in the electronic distribution, characteristic of molecules with inhibitory power. Almost all molecules determined, excepting one, contain oxygen atoms in their structure. It is clear there is no relationship between the concentration of the molecule in the extract and the compound with the greatest inhibitory character, likewise, the inhibition effect can be caused by the adsorption of more than one compound on the surface.

Table 1. ECMP extract GC-MS analysis.

Formula	Name	Retention time, min	%Area
$C_{10}H_{22}O$	1-Decanol	2.867	3.11
$C_3H_8O_3$	Propane-1,2,3-triol	3.415	6.40
C_6H_6O	Phenol	3.515	6.55
$C_4H_6O_3$	Acetoacetic acid	3.706	0.90
$C_6H_{10}O$	Cyclohexanone	9.200	5.57
$C_{14}H_{22}O$	4-*n*-Octylphenol	13.071	3.66
$C_{31}H_{48}O_2$	Fitonadiol	13.612	3.44
$C_{18}H_{36}O$	Octadecan	15.304	11.02

Formula	Name	Retention time, min	%Area
$C_{16}H_{32}O_2$	Palmitic acid	16.786	6.33
$C_{18}H_{34}O_2$	Oleic acid	18.540	4.18
$C_{21}H_{40}O$	2-Hydroxy-2-methyl-3-eicosyne	20.319	2.88
$C_{20}H_{26}$	3,4-Dimethyl-3,4-diphenylhexane	20.488	1.75

It was reported that phenolic compounds may form complex structures as protective films on the surface metal, which reduce corrosion [37]. Plant extracts are of interest for the production of compounds as corrosion inhibitors [38].

The extract composition determined by GC-MS does not include some compounds already reported in aqueous extract of banana peel evaluated previously [20]: gallocatechin ($C_{15}H_{14}O_7$) and catechin ($C_{14}H_{14}O_6$), classified as flavonoids with antioxidant properties. These are aromatic compounds. The present extract was obtained using a different methodology and ethanol as a solvent. It is clear the major components of an extract do not have to be the active components as inhibitors, on the other hand, components with an inhibitory effect can be in low concentrations in an extract, here may be interaction between them.

3.2. Weight loss (WL)

The WL evaluation was performed at 298 K, in the absence and presence of ECMP and ECMP–KI at different concentrations for six days. The data of efficiency and corrosion rate (W_{corr}) for the ECMP extract are shown in Table 2. Table 3 shows the data of efficiency and corrosion rate (W_{corr}) for the ECMP–KI. It can be seen the efficiency of inhibition increases with the increase in the concentration of the ECMP extract, reaching the higher efficiency (91%) at concentration of 1000 ppm. If KI is added (ECMP–KI), maximum efficiency reaches 93%. It confirms the synergic effect of KI addition, although in small extent.

Table 2. ECMP extract concentration, steel WL and inhibitor efficiency determined in 1 M HCl solution.

Concentration ECMP extract, ppm	W_{corr}, mg/cm^2·h	η%
0	30.106	0
200	7.775	74
400	6.209	79
600	4.672	84
800	3.816	87
1000	2.637	91

Table 3. ECMP extract concentration, steel WL and inhibitor efficiency determined in 1 M HCl solution in the presence of 100 ppm KI.

Concentration, ppm	W_{corr}, mg/cm^2·h	η%
0	30.106	0
200	6.562	78
400	5.323	82
600	4.083	86
800	3.194	89
1000	2.161	93

An increase in ECMP extract concentration determines a decrease in corrosion rate, reaching the lowest corrosion rate of 2.637 mg/cm^2 h at a concentration of 1000 ppm (Figure 2a). In case of KI addition, Figure 2b shows a decrease in corrosion rate reaching the lowest corrosion rate of 2.161 mg/cm^{2}h at a concentration of 1000 ppm of ECMP extract. It implies that the ECMP extract inhibits corrosion in SAE 1010 steel in 1 M HCl solution and, in the case of ECMP–KI extract, inhibition power increases a little more.

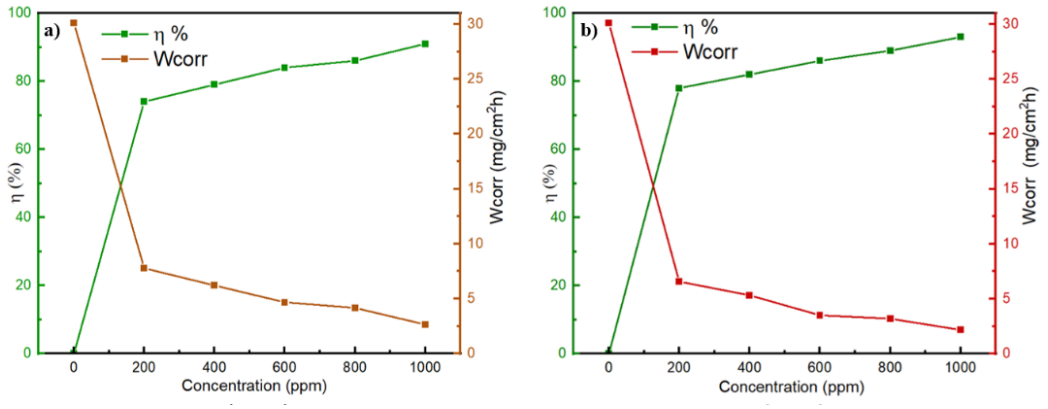

Figure 2. Inhibitory efficiency (η) and Wcorr *vs.* ECMP extract concentration : a) ECMP extract; b) ECMP–KI extract.

3.3. Electrochemical impedance spectroscopy (EIS)

Nyquist diagrams for steel in the presence of different ECMP extract concentrations are presented for three immersion times: 1 h (Figure 3a), 24 h (Figure 3b) and 48 h (Figure 3c). With respect to the blank solution, the radio of the semicircles increases according to the increase in the concentration of the extract. The data obtained were adjusted to the equivalent circuit proposed using the Z_{sim} software.

After adding the KI solution to the corrosive medium in the presence of the ECMP extract, the Nyquist diagrams were obtained for the same concentrations and immersion times: 1 h (Figure 3d), 24 h (Figure 3e) and 48 h (Figure 3f).

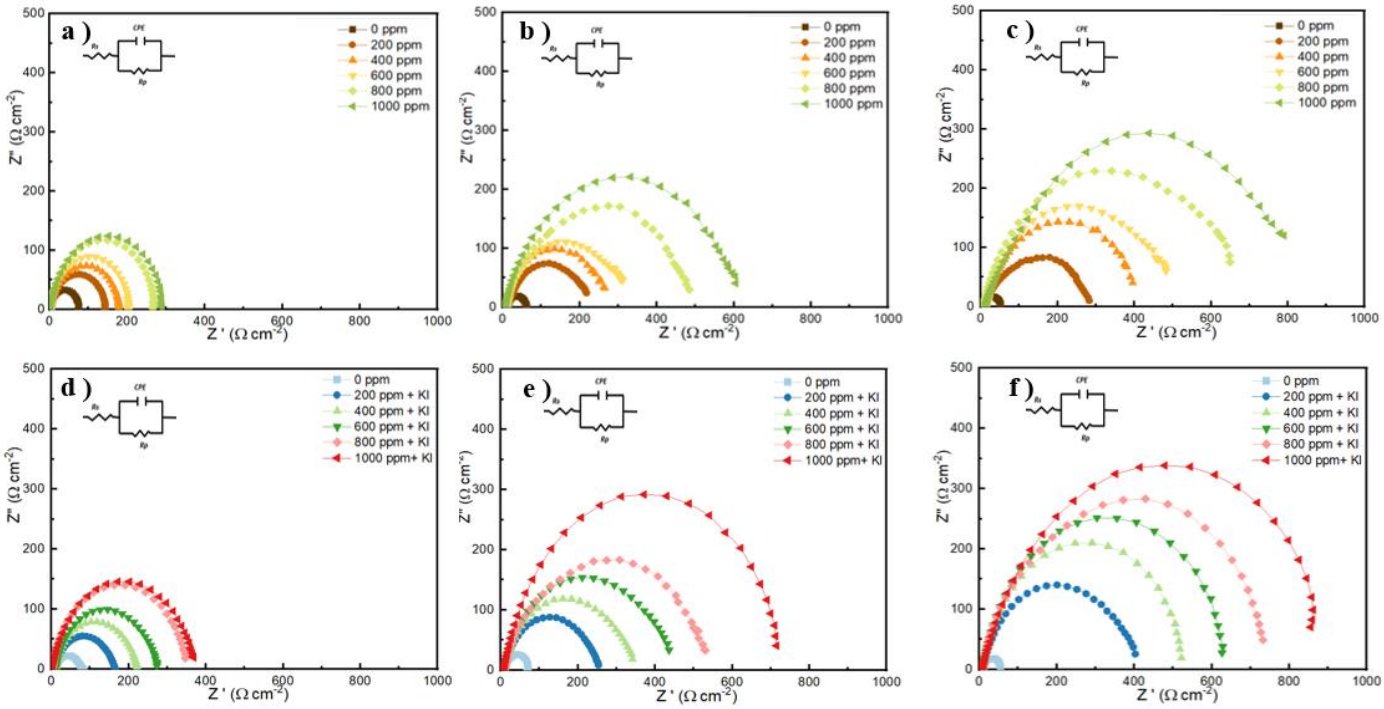

Figure 3. Nyquist diagrams of steel in 1 M HCl solution at different concentrations of ECMP extract in three immersion times: (a) 1 h, (b) 24 h and (c) 48 h. ECMP–KI extract concentrations in three immersion times: (d) 1 h, (e) 24 h and (f) 48 h.

According to Table 4, the maximum efficiency for the ECMP extract determined for the three immersion times is t_1 = 75%, t_2 = 89% and t_3 = 93%.

Table 4. R_{ct} and *IE* of 1010 steel in 1 M HCl solution at different ECMP extract concentrations at three immersion times: t_1 = 1 h, t_2 = 24 h, t_3 = 48 h.

Concentration ECMP extract, ppm	R_{ct} t_1, Ω·cm²	η t_1%	R_{ct} t_2, Ω·cm²	η t_2%	R_{ct} t_3, Ω·cm²	η t_3%
0	74	0	64	0	53	0
200	140	47	208	69	269	80
400	177	58	255	75	383	86
600	201	63	302	79	469	89
800	267	72	438	85	637	92
1000	291	75	600	89	767	93

On the other hand, the increases in η for the ECMP–KI extract obtained at the immersion times of 1 h, 24 h and 48 h, are 80%, 91% and 94%, respectively, as it is shown in the Table 5.

Table 5. R_{ct} and efficiency of SAE 1010 steel in HCl 1 M solution at different ECMP extract concentrations in presence of KI at three immersion times.

Concentration ECMP–KI extract (ppm)	R_{ct} t_1, Ω·cm²	η t_1%	S_1 t_1	R_{ct} t_2, Ω·cm²	η t_2%	S_1 t_2	R_{ct} t_3, Ω·cm²	η t_3%	S_1 t_3
0	74	0	0	64	0	0	53	0	0
200 + KI	165	55	1.09	253	75	1.03	403	87	1.08
400 + KI	222	67	1.36	341	81	1.14	522	90	1.12
600 + KI	273	73	1.50	436	85	1.21	627	92	1.14
800 + KI	347	79	1.64	531	88	1.25	732	93	1.16
1000 + KI	368	80	1.66	715	91	1.30	856	94	1.17

Comparing Tables 4 and 5, it is observed that for 1000 ppm ECMP extract concentration t_1, the efficiency increased with the synergistic additive from 75% to 80%, at t_2 from 89% to 91% and at t_3 from 93% to 94%. The increase in efficiency is relatively poor. It should be considered that IE obtained without KI is already high.

IE increases slightly with the addition of iodide ions to the solution containing ECMP extract, as well as the degree of coverage of the surface, in general, the condition of $S_1 > 1$ is met, which shows a small synergistic effect of I^- ions [39, 40], perhaps due to the high efficiency that is achieved without the addition of KI. Increasing the immersion time increases the efficiency, being higher when KI is added. However, the increase in efficiency is more significant at time t_1 than at times t_2 and t_3.

The presence of loops (helical shape) indicates the corrosion of steel in acid solution is controlled by the charge transfer process at the electrode-solution interface [41]. The increase in the diameter of the loops in the Nyquist diagram indicates the formation of a more capacitive film on the metal surface, favoring the formation of a protective layer [42].

Table 6 shows some research carried out with *Musa paradisiaca*. We can see the IE reported in the present paper is slightly higher, exceeding the efficiency of 90%. There are different types of *Musa paradisiaca* extracts: aqueous, ethanolic, acetonic, peel and leaf. Table 6 shows the efficiencies according to the type of specimen, extract and medium. They are not large despite the fact that the extracts, specimens and environments are different.

The inhibitory capacity of the extracts is always present, despite using different procedures, different parts of the plant and solvents. Considering that only a minimum concentration of the inhibitory compounds is required to be effective, their presence in all the extracts makes it possible to determine a marked inhibitory character of these compounds for all the environments tested.

Table 6. *Musa paradisiaca* as corrosion inhibitor. Literature reports and data corresponding to the present paper.

Specimen	Corrosive solution	Extract concentration (ppm)	η%	Reference
Musa paradisiaca peel (acetone extract)	1 M HCl	300	89–90	[20]
*Musa paradisiaca l*eaf (aqueous extract)	0.5 M H_2SO_4	3000	81.9	[21]
Musa paradisiaca leaf (aqueous extract)	Seawater	1000	86.51	[22]
Musa paradisiaca peel (aqueous extract)	0.1 M HCl	500	87	[23]
Musa paradisiaca peel (ethanolic extract)	1 M HCl	1000	91–93*	This work

*Efficiency (η) range for 48 h time of immersion in the three evaluation techniques used (WL, EIS, PDP).

When KI is added to the ECMP extract solution, iodide ions are formed. Some sites on the surface of SAE 1010 steel may be positively charged. I^- ions are adsorbed on such sites on the metal surface and change the interfacial activity, while ECMP extract compounds may be responsible for the hydrophobic behavior in acid solution [43].

The increased efficiency of the inhibitor is observed due to the interaction of the inhibitor components on the surface and the possible interaction of the positively charged molecules of the inhibitor with the negative I^- ions adsorbed on the surface. The addition of KI to ECMP extract increases efficiency over using ECMP extract alone.

Table 7 shows the published synergistic additives, noting that the halide most used for the synergistic effect is KI over KBr and KCl. The amounts used vary depending on the specimen to be studied. However, the efficiency can vary from 3% to 32%, while the addition of the KI of this work produced an increase of 14%. The synergistic additive concentration for this work was 100 ppm of a 0.5 mM KI solution which is lower than other reports presented in Table 7.

Surface adsorption mechanism in the presence of iodide ions is shown in Equations 12, 13 and 14. The existence of I^- in an acid medium increases η of some organic compounds. Iodide anions are adsorbed on the iron surface and facilitate the arrival of organic cations to the surface, resulting in an increase in surface coverage [32, 47].

Similar studies have shown impedance data increases at shorter immersion times. When immersion time increases, R_{ct} gradually decrease until reaching a constant range, which is attributed to rapid inhibitor adsorption and diffusion of the electrolyte over time [40].

Table 7. Previous reports on the use of synergic additives and results of the present paper.

Specimen	Corrosive solution	Extract concentration, ppm	η%	Additive	η with additive %	Reference
Rice husk	1 M H_2SO_4	1250	70	0.3 mM KI	79	[32]
Goma arábiga	0.5 M H_2SO_4	2000	50	0.1 mM KBr	57	[42]
				0.1 mM KCl	62	
				0.5 mM KI	98	
Cortex *Schinus molle*	0.5 M H_2SO_4	3000	62	2 mM KI	94	[44]
Mangrove tannin	0.5 M HCl	3000	89		94	[45]
Mimosa tannin		3000	82	0.1 mM KI	94	
Chestnut tannin		2000	73		93	
Leves *morus alba pendula*	1 M HCl	400	93	10 mM KI	96	[46]
Pennisetum purpureum	3.5% HCl	5000	91	1 mM KI	96	[29]
Peel *Musa paradisiaca*	1 M HCl	1000	80	0.5 mM KI	94	This work

$$Fe + H_2O + I^- \rightleftharpoons (FeI^-OH)_{ads} + H^+ + \bar{e} \quad (12)$$

$$F(FeOH)_{ads} \rightleftharpoons (FeI^-OH)^+ + \bar{e} \quad (13)$$

$$(FeI^-OH) + H^+ \rightleftharpoons Fe^{2+} + I^- + H_2O \quad (14)$$

According to the literature, changes in inhibitor composition can increase stability and performance [27], the limitation for a complete understanding of the mechanism of corrosion inhibition by organic inhibitors lies in the concentration ranges and the difficulty to monitor the process at the fluid interface-metal [33].

Table 8 shows surface area coverage (θ) and double layer capacitance (C_{dl}) determined for the three immersion times at different concentrations of ECMP extract.

The coverage degree increases with the immersion time, reaching maximum values for t_1 = 0.75, t_2 = 0.89 and t_3 = 0.93. The increase in R_{ct} is attributed to the increase in surface coverage of ECMP extract molecules on the electrode surface. The double layer capacitance decreases with time: t_1 = 4.42, t_2 = 1.20 and t_3 = 0.71 (μF/cm^2).

Table 8. Surface coverage (θ) and double layer capacitance (C_{dl}) determined at different ECMP extract concentrations and three times of immersion.

Concentration ECMP extract, ppm	θ t_1	C_{dl} t_1, μF/cm²	θ t_2	C_{dl} t_2, μF/cm²	θ t_3	C_{dl} t_3, μF/cm²
0	0	65.77	0	134.44	0	196.40
200	0.47	19.11	0.69	10.27	0.80	7.12
400	0.58	12.22	0.75	6.313	0.86	2.90
600	0.63	8.877	0.79	4.778	0.89	2.00
800	0.72	5.11	0.85	2.11	0.92	1.09
1000	0.75	4.42	0.89	1.20	0.93	0.71

Table 9 shows surface area coverage (θ) and double layer capacitance (C_{dl}), for the three immersion times at different concentrations of ECMP–KI extract.

The coverage degree increases with the immersion time, reaching maximum values for $t_1 = 0.80$, $t_2 = 0.91$ and $t_3 = 0.94$. The increase in R_{ct} is attributed to the increase in surface coverage of ECMP extract molecules on the electrode surface. The double layer capacitance decreases with time: $t_1 = 3.77$, $t_2 = 0.908$ and $t_3 = 0.55$ (μF/cm²) [48].

Table 9. Surface coverage (θ) and double layer capacitance (C_{dl}) determined at different ECMP extract concentrations in presence of 100 ppm KI and three times of immersion.

Concentration ECMP extract, ppm	θ t_1	C_{dl} t_1, μF/cm²	θ t_2	C_{dl} t_2, μF/cm²	θ t_3	C_{dl} t_3, μF/cm²
0	0	88.89	0	78.93	0	78.93
200	0.52	20.6	0.72	8.682	0.86	3.82
400	0.64	11.28	0.79	5.243	0.9	1.45
600	0.71	7.97	0.84	3.428	0.91	1.01
800	0.77	4.26	0.86	1.98	0.93	0.77
1000	0.78	3.77	0.9	0.908	0.94	0.55

The decrease in C_{dl} and the increase in R_{ct} are attributed to the adsorption of molecules with the inhibition effect on the metal surface what, cause a decrease in the dielectric constant and/or to the increase in the electrical double layer [49]. The relative electroactive area (REA) was calculated using Equation 15. Figure 4 shows the relationship between R_{ct} and REA for the ECMP extract (Figure 4a) and ECMP–KI extract (Figure 4b).

$$\text{REA} = 1 - \theta \tag{15}$$

where $\theta = \eta/100$; θ = coverage degree.

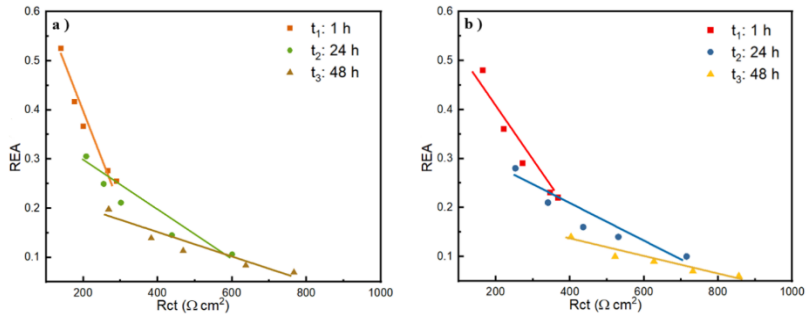

Figure 4. REA vs R_{ct} at different immersion times in presence of (a) ECMP extract and (b) ECMP + KI extract.

R_{ct} can be used to characterize the degree of charge transfer difficulty occurring in the solution-steel interface. ECMP extract molecules create an adsorbed film on the surface. The increase in R_{ct} with increasing ECMP extract concentration can be attributed to the increase in surface coverage by ECMP extract molecules [50].

Therefore, θ increases with increasing ECMP extract concentration (Figure 4a). All points, regardless of time, show a tendency to decrease REA as R_{ct} increases. C_{dl} could be related to metal-solution reactions, since there is an increase in the coverage of the ECMP extract molecule on the metal, which causes a decrease in the dissolution of the metal [51].

3.4. Potentiodynamic polarization curves (PDP)

PDP curves of SAE 1010 carbon steel were determined in the absence and presence of five concentrations of ECMP extract in 1 M HCl solution at room temperature, at immersion times of: t_1 = 1 h, t_2 = 24 h and t_3 = 48 h.

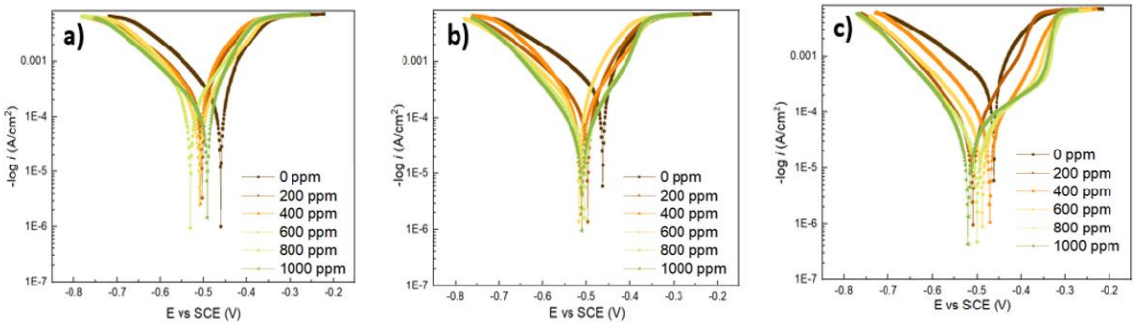

Figure 5. Tafel polarization curves for steel at different ECMP extract concentrations and immersion time: a) 1 h, b) 24 h and c) 48 h.

Tafel curves are presented in Figure 5 for steel in the presence of ECMP extract, it is observed a decrease in corrosion current as ECMP extract concentration increases, compared to the blank curve. The corrosion potentials are less positive than the blank (Figure 5a, 5b and 5c). The cathodic and anodic branches of Tafel curves lie below the reference curve of the blank solution. The inhibitor forms a film on the metal surface and blocks the formation

of both anodic and cathodic active sites, the change in the Tafel curve increases with the concentration of the extract; it reflects a decrease in the I_{corr} value, that is, the rate of corrosion decreases [52, 53].

Table 10 shows the electrochemical parameters, calculated from the Tafel polarization curves; corrosion potential (E_{corr}), current density (I_{corr}), anodic (β_a) and cathodic (β_c) Tafel slope, inhibitory efficiency (η) and coverage area (θ) at five different ECMP extract concentrations respecting the blank solution.

For immersion times t_1, t_2 and t_3, with respect to the blank (0 ppm), the addition of ECMP extract in HCl solution reduces the intensity of the corrosion current. At a concentration of 1000 ppm, the corrosion current density (I_{corr}) is $t_1 = 4.51$, $t_2 = 3.56$ and $t_3 = 3.22$ Acm^{-2}. The respective corrosion potential (E_{corr}) is $t_1 = -491$, $t_2 = -509$ and $t_3 = -519$ mV.

Table 10. Changes in E_{corr}, I_{corr}, β_a, β_c, IE (η) and coverage degree (θ) of steel in acid medium with and without addition of ECMP extract.

Concentration of the ECMP–KI extract, ppm	Immersion times, h	$-E_{corr}$, mV	I_{corr}, μA·cm^{-2}	β_a, mV/dec	β_c, mV/dec	η%	θ
0	1	461	19.17	0.12	0.17	0	0.00
	24	463	32.98	0.28	0.49	0	0.00
	48	464	36.9	0.43	0.61	0	0.00
200	1	503	10.63	0.72	1.10	45	0.45
	24	496	14.76	0.51	2.21	55	0.55
	48	508	16.11	0.55	1.92	56	0.56
400	1	511	9.63	0.71	1.11	50	0.50
	24	512	10.48	0.79	1.94	68	0.68
	48	472	11.48	1.09	1.19	70	0.70
600	1	510	7.76	0.66	1.16	59	0.59
	24	516	8.8	0.93	1.98	73	0.73
	48	488	9.25	0.83	1.36	75	0.75
800	1	538	5.33	0.71	1.24	72	0.72
	24	503	6.41	0.79	1.22	80	0.8
	48	500	6.84	0.88	0.82	81	0.81
1000	1	491	4.51	0.87	1.43	76	0.76
	24	509	3.56	0.92	1.03	89	0.89
	48	519	3.22	0.97	0.74	91	0.91

Tafel curves are shown in Figure 6 for steel in the presence of ECMP–KI extract. A change is observed as ECMP–KI extract concentration increases compared to the blank curve. The corrosion potentials are more negative than the blank (Figures 6a, 6b and 6c).

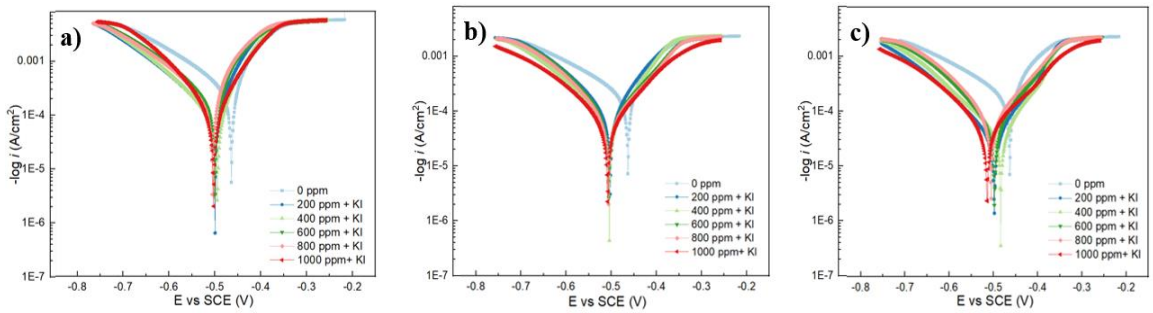

Figure 6. Tafel polarization curves for steel at different ECMP extract concentrations with the addition of 100 ppm KI at three immersion times: a) 1 h, b) 24 h and c) 48 h.

Table 11 shows the electrochemical parameters calculated from Tafel polarization curves at different ECMP–KI extract concentrations.

In the case of the immersion times t_1, t_2 and t_3, the addition of ECMP extract in HCl solution reduces the intensity of the corrosion current. At a concentration of 1000 ppm, the corrosion current density is I_{corr} $t_1 = 4.24$ μA·cm^{-2}, I_{corr} $t_2 = 3.74$ μA·cm^{-2} and I_{corr} $t_3 = 3.60$ μA·cm^{-2}. The respective corrosion potentials are: E_{corr} $t_1 = -503$ mV, E_{corr} $t_2 = -508$ mV and E_{corr} $t_3 = -513$ mV.

Table 11. Changes in E_{corr}, I_{corr}, β_a, β_c, IE (η) and coverage degree (θ) of steel in acid medium with and without addition of ECMP–KI extract.

Concentration ECMP–KI extract, ppm	Immersion times, h	$-E_{corr}$, mV	I_{corr}, μA·cm^{-2}	β_a, mV/dec	β_c, mV/dec	η%	θ
0	1	461	19.17	0.126	0.175	0	0.00
	24	463	32.98	0.279	0.488	0	0.00
	48	464	36.90	0.426	0.608	0	0.00
200	1	499	9.79	0.517	0.138	49	0.49
	24	505	13.84	0.896	0.114	58	0.58
	48	497	14.98	0.935	0.150	59	0.59
400	1	495	9.50	0.75	0.106	50	0.50
	24	504	9.99	0.927	0.140	70	0.70
	48	483	11.03	0.927	0.156	70	0.70
600	1	499	7.10	0.769	0.122	63	0.63
	24	505	8.32	0.951	0.111	75	0.75
	48	498	9.02	0.984	0.126	76	0.76

Concentration ECMP–KI extract, ppm	Immersion times, h	$-E_{corr}$, mV	I_{corr}, μA·cm^{-2}	β_a, mV/dec	β_c, mV/dec	η%	θ
800	1	506	4.87	0.697	0.083	75	0.75
	24	505	6.40	0.974	0.112	81	0.81
	48	505	5.89	0.955	0.113	84	0.84
1000	1	503	4.24	0.720	0.760	78	0.78
	24	508	3.04	0.880	0.110	91	0.91
	48	513	2.76	0.951	0.108	93	0.93

In the presence of ECMP extract, the corrosion potential (E_{corr}) is shifted towards the anodic region. The anodic curve is responsible for the oxidation of the metal, while the cathodic curve is responsible for the evolution of hydrogen in the acid medium; however, to determine the type of inhibitor, the displacement must be less than ±85 mV. According to the E_{corr} results, ECMP extract is a mixed type inhibitor with a value for $t_1 = \pm 42$, $t_2 = \pm 42$ and $t_3 = \pm 49$, which reduces the phenomenon of corrosion. It is caused by the adsorption of ECMP extract molecules on the surface of the mild steel.

The significant reduction in corrosion current density (I_{corr}) indicates a decrease in corrosion and an increase in the efficiency with ECMP–KI extract. The anodic (β_a) and cathodic (β_c) slopes do not change significantly, suggesting that there is no change in the corrosion mechanism [53]. On the other hand, the efficiency increases with the immersion time. In the presence of 1000 ppm of ECMP extract, the efficiencies were 76%, 89% and 91% at 1 h, 24 h and 48 h, respectively, but in the presence of 1000 ppm of the ECMP extract and 100 ppm of KI, they were 78%, 91%, and 93%, at the same times. These types of inhibitors form a barrier or film on the metal surface, attenuating the corrosion process and modifying the speed of the anodic-cathodic reactions, decreasing the arrival or departure of species from the metal surface, or increasing the electrical resistance on the metal surface [54, 55].

3.5. Surface Characterization

Morphological changes on the metal surface were monitored using a scanning electron microscope (SEM). The elemental composition of the surface was determined by EDX characterization at 48 h of immersion time. Figure 7a shows the morphology of polished steel before being exposed to the HCl corrosive environment, the steel does not show damage or cracks, however, when it is immersed in the 1 M HCl solution, the surface becomes rough (Figure 7b). When 1000 ppm of ECMP extract is added, the damage observed on the steel surface is lower (Figure 8c). When 1000 ppm of ECMP extract and 100 ppm of KI solution are added, the damage on the steel surface is even lower. It means that the ECMP extract inhibitor contains compounds that adsorb and, in turn, minimize the formation of corrosive products on the steel surface, which in turn with the presence of KI increases a small

percentage of efficiency. The surface charges on the metal induce the occurrence of the corrosion phenomenon and, at the same time, favor the adsorption of chloride ions from the HCl solution [56, 57].

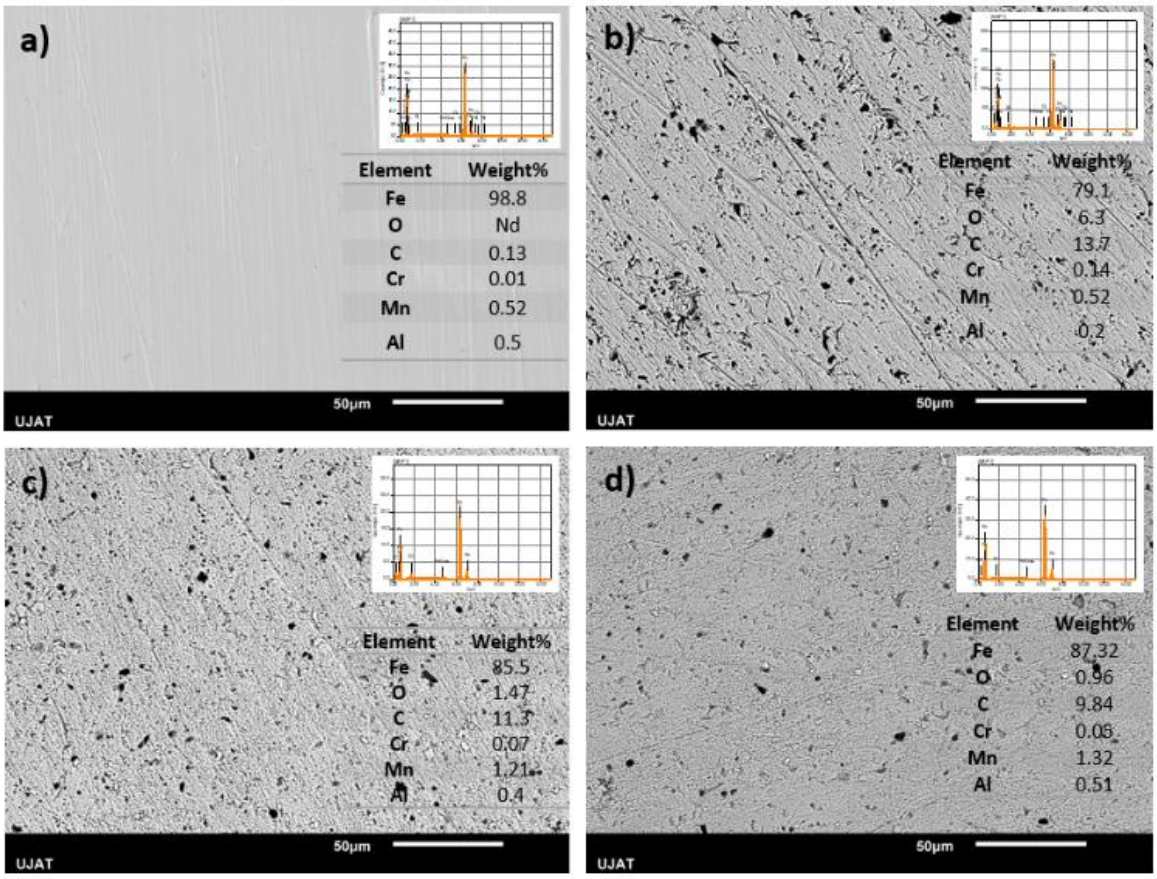

Figure 7. SEM and EDX a) clean and polished steel surface, b) steel surface after immersion in HCl solution during 48 h, c) steel surface after immersion in HCl solution containing 1000 ppm ECMP extract, d) steel surface after immersion in HCl solution containing 1000 ppm ECMP extract and 100 ppm KI.

3.6. Adsorption Isotherms

To understand the interaction mechanism at the interface of ECMP extract molecules with the metal surface, it is necessary to determine which adsorption isotherm model fits best. Calculations were made using Equations 8, 9 and 10 cited in the methodology for the Langmuir, Temkin and Freundlich isotherms. Figures 8a, 8b, and 8c show the results of statistical fitness obtained after processing data corresponding to EIS, PDP and WL according to the isotherm models evaluated, in presence of ECMP extract. In Figures 8d, 8e and 8f, the experimental data for the isotherms models evaluated using the above mentioned techniques in the presence of ECMP–KI extract are shown.

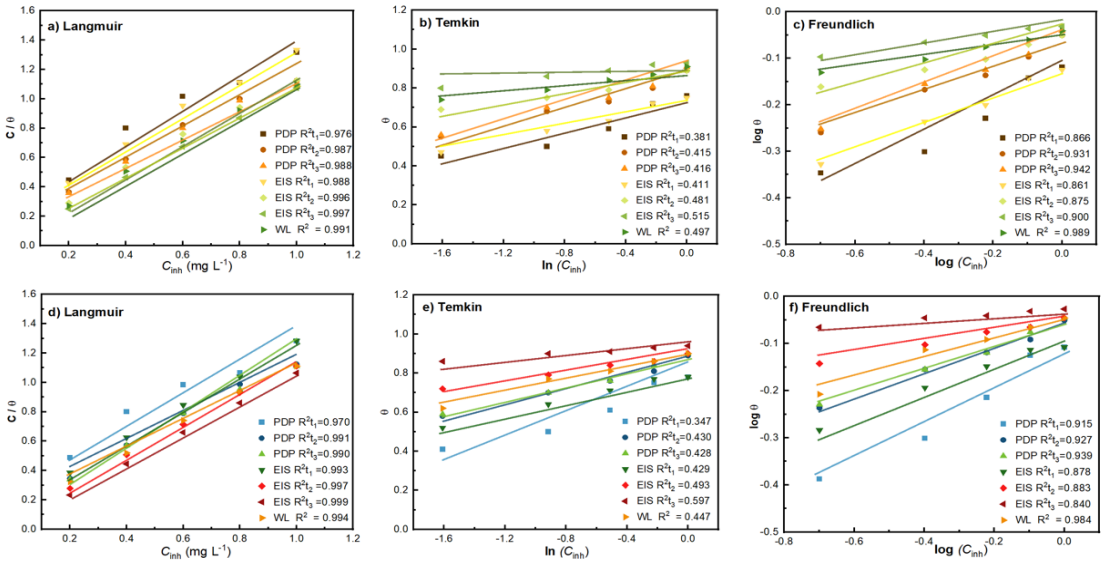

Figure 8. Adsorption isotherms of ECMP extract on steel fitted to the following models: Langmuir (a), Temkin (b) and Freundlich (c). Adsorption isotherms of ECMP extract in the presence of KI fitted to models: Langmuir (d), Temkin (e) and Freundlich (f).

Figures 8a and 8d show that the best fit of the data obtained by the electrochemical PDP technique corresponds to the Langmuir isotherm model. As can be seen in the figures, the corresponding correlation coefficients (R^2) are: ECMP$t_{1\ (PDP)}$ = 0.976, ECMP$t_{2\ (PDP)}$ = 0.987 and ECMP$t_{3\ (PDP)}$ = 0.988. In case of the additional presence of KI: ECMP–KI$t_{1\ (PDP)}$ = 0.970, ECMP–KI$t_{2\ (PDP)}$ = 0.991 and ECMP–KI$t_{3\ (PDP)}$ = 0.990. Using EIS technique, the corresponding correlation coefficients are, in the presence of ECMP, for ECMP$t_{1\ (EIS)}$ = 0.988, ECMP$t_{2\ (EIS)}$ = 0.986 and ECMP$t_{3\ (EIS)}$ = 0.997. In the presence of KI the coefficients are ECMP–KI$t_{1\ (EIS)}$ = 0.993, ECMP–KI$t_{2\ (EIS)}$ = 0.997 and ECMP–KI$t_{3\ (EIS)}$ = 0.999. With the technique WL, the following correlation coefficient were obtained: ECMP$_{(WL)}$ = 0.991 and ECMP–KI$_{(WL)}$ = 0.994. In the Temkin isotherm model of Figures 8b and 8e, (R^2) is in the range from 0.381 to 0.515 in the presence of ECMP extract at different times by using different techniques. Respecting the Temkin isotherm model (Figure 8b and 8e), (R^2) in presence of ECMP extract is in the range from 0.381 to 0.515 at different times and by using different techniques applied. In case of ECMP–KI extract, (R^2) is in the range from 0.347 to 0.597 at different times and by using different techniques applied. In the Freundlich isotherm model (Figures 8c and 8f), (R^2) in the presence of ECMP extract is in the form range from 0.861 to 0.989 at different times and by using different techniques. For ECMP–KI extract, (R^2) is in the range from 0.840 to 0.984 at different times and using different techniques applied.

The above results indicate that the best model represented by the experimental data, is the Langmuir adsorption isotherm. According to other authors, they establish that there is a formation of a protective monolayer on the surface of the metal, this is due to the adsorption of the organic molecules of ECMP extract and ECMP–KI extract on the metal surface, and forming a film [58]. However, it is observed that there are no significant differences between

the fittings to the Langmuir model in the presence or not of KI because the effect of the KI additive is very small. Therefore, this shows that increasing the concentration from 200 to 1000 ppm varies linearly to the adsorption of ECMP extract and ECMP–KI extract molecules on the metal surface, because there is a strong affinity of inhibitor molecules [59].

Table 12 shows the adsorption parameters obtained, the intercept and the slope obtained by PDP and EIS techniques and by WL. The R^2 values obtained confirm that the best adsorption isotherm is the Langmuir model. The slope values determined for the three models of adsorption isotherms using the PDP and EIS techniques in the presence of ECMP extract and ECMP–KI extract show positive signs, indicating a positive correlation, otherwise, when the slope values are negatives, they indicate a negative correlation [57–59].

The equilibrium adsorption constant (K_{ads}) for the Langmuir isotherm can be calculated using the EIS, PDP and WL data shown in Table 13. In the PDP data it is observed that K_{ads} increases with immersion time, varying the ECMP extract from 0.974 to 1.053. The ECMP–KI extract ranges from 1.014 to 1.078. The EIS K_{ads} data increase with immersion time, which varies the ECMP extract is from 0.894 to 0.971 and the ECMP–KI, extract varies is from 0.905 to 0.962. WL data, K_{ads} increases from ECMP extract = 0.966 to ECMP–KI extract = 1.007.

The increase in K_{ads} is attributed to the strong adsorption capacity of the molecules of the ECMP–KI extract on the surface of the metal. It can also be considered as a measure of the adsorption forces between the inhibitor molecules to the solution of the surface of the metal [60, 61].

4. Conclusions

Compounds identified by GC-MS analysis as phenols, palmic acid, octadecan and propane-1,2,3-triol and others are molecules with potential corrosion-inhibiting properties. In this work, the chemical composition of the extract shows the presence of heterocyclic compounds, particularly phenols. It is very likely that the inhibitory properties are produced by a mixture of different molecules, since almost all of them could have inhibitory properties acting independently. Different extracts of the same product show inhibitory properties as reported in the literature. It means the molecules or mix of molecules contained in the extracts are of the same type, having similar inhibitory properties.

The ECMP ethanolic/water extract shows excellent performance as a corrosion inhibitor of 1010 steel in HCl. The determination of WL, EIS and PDP showed an efficiency of 75% to 93% at an immersion time of 48 h. Electrochemical techniques show that η increases with immersion time and that the inhibitor has a mixed behavior, influencing both branches of the polarization curve. The addition of KI shows an increase in efficiency from 80 to 94% at an immersion time of 48 h, probably because the adsorption of ECMP extract on the steel surface is very high, reaching a high degree of surface saturation. The Langmuir adsorption isotherm is the model that best fits the experimental data for the adsorption of ECMP extract and for ECMP–KI extract on the steel surface. The addition of the halide (KI) allowed the increase in inhibition at concentrations of 1000 ppm, with greater efficiency for t_3.

Table 12. Adsorption parameters obtained by PDP, EIS and WL, for the three types of isotherm models in three different immersion times (where Int. means intercept).

Extract	Isotherm model	Immersion time, h	Technique PDP			Technique EIS			Technique WL in immersion times of 6 days		
			R^2	Int.	Slope	R^2	Int.	Slope	R^2	Int.	Slope
ECMP	Langmuir	1	0.976	0.321	1.026	0.988	0.231	1.118	0.991	0.08	1.035
		24	0.987	0.199	0.965	0.996	0.106	1.037			
		48	0.988	0.193	0.949	0.997	0.05	1.027			
	Temkin	1	0.381	0.734	0.200	0.411	0.744	0.175	0.497	0.897	0.103
		24	0.415	0.859	0.198	0.481	0.873	0.122			
		48	0.416	0.877	0.201	0.515	0.933	0.082			
	Freundlich	1	0.866	–0.13	0.342	0.934	–0.123	0.292	0.878	–0.046	0.126
		24	0.931	–0.061	0.284	0.986	–0.057	0.156			
		48	0.942	–0.052	0.282	0.964	–0.029	0.095			
ECMP–KI	Langmuir	1	0.970	0.367	0.927	0.993	0.172	1.104	0.977	0.128	0.993
		24	0.991	0.171	0.986	0.997	0.08	1.045			
		48	0.990	0.175	0.962	0.998	0.028	1.039			
	Temkin	1	0.347	0.767	0.242	0.429	0.793	0.168	0.347	0.168	0.011
		24	0.430	0.866	0.182	0.493	0.892	0.108			
		48	0.428	0.88	0.188	0.537	0.939	0.048			
	Freundlich	1	0.915	–0.107	0.422	0.878	–0.095	0.261	0.978	–0.041	0.225
		24	0.927	–0.058	0.254	0.883	–0.048	0.135			
		48	0.939	–0.051	0.258	0.840	–0.026	0.054			

Table 13. Calculations of the equilibrium adsorption constant (K_{ads}) for the Langmuir isotherm model.

Extract	Type of evaluation	Immersion time, h	K_{ads}, L/mol
ECMP	PDP	1	0.974
	PDP	24	1.036
	PDP	48	1.053
	EIS	1	0.894
	EIS	24	0.964
	EIS	48	0.971
	WL	1	0.966
ECMP–KI	PDP	1	1.078
	PDP	2	1.014
	PDP	48	1.039
	EIS	1	0.905
	EIS	2	0.956
	EIS	48	0.962
	WL	1	1.007

Acknowledgement

We are grateful to the Universidad Juarez Autonoma de Tabasco and the Universidad Autonoma de Campeche for their availability of time to carry out the research, as well as CONAHCYT for the scholarship granted to carry out the Doctorate in Engineering Sciences at the Universidad Juarez Autonoma de Tabasco.

References

1. M. Zhang, Davidian involucrata leaves extract as green corrosion inhibitor for low carbon steel in concrete pore solution containing chloride ions, *Int. J. Electrochem. Sci*., 2021, **16**, 21042. doi: 10.20964/2021.04.01
2. H.A. Al-Moubaraki and I.B. Obot, Top of the line corrosion: causes, mechanisms, and mitigation using corrosion inhibitors, *Arabian J. Chem*., 2021, **14**, 103116. doi: 10.1016/j.arabjc.2021.103116
3. A. Fateh, M. Aliofkhazraei and A.R. Rezvanian, Review of corrosive environments for copper and its corrosion inhibitors, *Arabian J. Chem*., 2020, **13**, 481–544. doi: 10.1016/j.arabjc.2017.05.021
4. Z.M. Away, A.N. Abd and K.H. Hassan, Corrosion prevention of AA2024-T3 aluminum alloy in acidic media using Cydonia Vulgaris leaves extract, *Int. J. Corros. Scale Inhib*., 2023, **12**, 48–60. doi: 10.17675/2305-6894-2023-12-1-3

5. A. El Yadini, H. Saufi, E. Perez, M. Blanzat, S. Franceschi-Messant and S. El Hajjaji, Synthesis and characterization of bolaform surfactants from sugar derivative and their associates with 2-aminobenzimidazole as inhibitor of zinc in 3% NaCl medium, *Int. J. Corros. Scale Inhib*., 2020, **12**, 32–47. doi: 10.17675/2305-6894-2023-12-1-2
6. X. Rao, L. Zhou, G. Zhang, X. Wang, S. Xia and L. Yu, Investigation of a hydrophobically associating AMAHS polyacrylamides: A new corrosion inhibitor for mild steel in HCl, *Mater. Corros*., 2020, **71**, 1521–1532. doi: 10.1002/maco.201911464
7. C. Verma, D.K. Verma, E.E. Ebenso and M.A. Quraishi, Sulfur and phosphorus heteroatom-containing compounds as corrosion inhibitors: An overview, *Heteroat. Chem*., 2018, **29**, no. 4, 1–20. doi: 10.1002/hc.21437
8. A.G. Berezhnaya, E.S. Khudoleeva and V.V. Chernyavina, Some imidazolines and their mixtures with inorganic anions as inhibitors of acid corrosion of steel, *Int. J. Corros. Scale Inhib*., 2021, **10**, 649–661. doi: 10.17675/2305-6894-2021-10-2-11
9. A. Mandujano, J. Morales, H. Herrera, L. Corona and J. Juárez, Evaluation of the electrochemical behavior of nopal extract (Opuntia Ficus-Indica) as a possible corrosion inhibitor, *Rev. of Metallurgy*., 2017, **53**, e108.
10. N.I. Nabilah, S. Sobri, Y.A. Yusof and N. Kassim, Oil palm empty fruit bunch extract and powder as an eco-friendly corrosion inhibitor for mild steel: A comparison study, *Mater. Corros*., 2019, **70**, 1111–1119. doi: 10.1002/maco.201910959
11. V. Saraswat and M. Yadav, Carbon Dots as Green Corrosion Inhibitor for Mild Steel in HCl Solution, *Chemistry Select*, 2020, **5**, 7347–7357. doi: 10.1002/slct.202000625
12. I.E. Ekere, O. Agboola, S.O.I. Fayomi, A.O. Ayeni and A.Ayodeji, Investigation of corrosion inhibition by Cassava leaf DNA on AIS 1015 low carbon steel in sodium chloride solution, *Int. J. Corros. Scale Inhib*., 2023, **12**, 424–437. doi: 10.17675/2305-6894
13. A.A. Al-Amiery, A. Kadhim, A. Al-Adili and Z.H. Tawfiq, Limits and developments in ecofriendly corrosion inhibitors of mild steel: a critical review. Part 1: Coumarins, *Int. J. Corros. Scale Inhib*., 2021, **10**, 1355–1384. doi: 10.17675/2305-6894-2021-10-4-1
14. K. Xhanari and M. Finšgar, Organic corrosion inhibitors for aluminum and its alloys in chloride and alkaline solutions: A review, *Arabian J. Chem*., 2019, **12**, 4646–4663. doi: 10.1016/j.arabjc.2016.08.009
15. D. Muliastri, D.E. Septiyani, N. Afif, V.T. Sirenden and J.N.R. Suprihartini, Application of Organic Inhibitors to the Corrosion of Materials AISI 1070 Steel, *International Journal Applied Technology Research*, 2021, **2**, 12–20. doi: 10.35313/ijatr.v2i1.39
16. T.K. Bhuvaneswari, C. Jeyaprabha and P. Arulmathi, Corrosion inhibition of mild steel in hydrochloric acid by leaves extract of Tephrosia purpurea, *J. Adhes. Sci. Technol*., 2020, **34**, 2424–2447. doi: 10.1080/01694243.2020.1766395
17. L. Ghayati, Y. Sert, N.K. Sebbar, Y. Ramli, N. Ahabchane, A. Talbaoui, J. Mague, B. Ibrahim, M. Labd, M. Essassi, N. Zaqri and A. Alsalme, Syntheses of novel 1,5-benzodiazepine derivatives: Crystal structures, spectroscopic characterizations,

Hirshfeld surface analyses, molecular docking studies, DFT calculations, corrosion inhibition anticipation, and antibacterial activities, *J. Heterocycl. Chem*., 2021, **58**, 270–289. doi: 10.1002/jhet.4167
18. J. Kaur, N. Daksh and A. Saxena, Corrosion Inhibition Applications of Natural and Eco-Friendly Corrosion Inhibitors on Steel in the Acidic Environment: An Overview, *Arabian J. Sci. Eng*., 2022, **47**, 57–74. doi: 10.1007/s13369-021-05699-0
19. L. Feng, S. Zhang, Y. Lu, B. Tan, S. Chen and L. Guo, Synergistic corrosion inhibition effect of thiazolyl-based ionic liquids between anions and cations for copper in HCl solution, *Appl. Surf. Sci*., 2019, **483**, 901–911. doi: 10.1016/j.apsusc.2019.03.299
20. G. Ji, S. Anjum, S. Sundaram and R. Prakash, *Musa paradisica* peel extract as green corrosion inhibitor for mild steel in HCl solution, *Corros. Sci*., 2015, **90**, 107–117. doi: 10.1016/j.corsci.2014.10.002
21. R. Mayanglambam, V. Sharma and G. Singh, *Musa paradisiaca* extract as a green inhibitor for corrosion of mild steel in 0.5 M sulphuric acid solution, *Port. Electrochim. Acta*, 2011, **29**, 405–417. doi: 10.4152/pea.201106405
22. R. Rosliza and A. Nurashimah, The Effectiveness of *Musa paradisiaca* as Green Inhibitor for Mild steel in Marine Corrosion, *J. Phys.: Conf. Se*., 2021, 1**874**, 012073. doi: 10.1088/1742-6596/1874/1/012073
23. C.B. Manikandan, S. Balamurugan, P. Balamurugan and S.L. Beneston, Corrosion inhibition of mild steel by using banana peel extract, *International Journal of Innovative Technology and Exploring Engineering*, 2019, **8**, 1372–1375.
24. P.R. Prabhu, P. Hiremath, D. Prabhu, M.C. Gowrishankar and B.M. Gurumurthy, Chemical, electrochemical, thermodynamic and adsorption study of EN8 dual-phase steel with ferrite-martensite structure in 0.5 M H_2SO_4 using pectin as inhibitor, *Chem. Pap*., 2021, **75**, 6083–6099. doi: 10.1007/s11696-021-01773-x
25. H. Kumar and V. Yadav, Highly efficient and eco-friendly acid corrosion inhibitor for mild steel: Experimental and theoretical study, *J. Mol. Liq*., 2021, **335**, 116220. doi: 10.1016/j.molliq.2021.116220
26. A.K.P. Setiman, A. Ridhova, G. Priyotomo, B. Elya, A. Maksum, Y. Sadeli S. Sutopo, T. Aditiyawarman, R. Riastuti, and J. Soedar, Development of white tea extract as green corrosion inhibitor in mild steel under 1 m hydrochloric acid solution, *East.-Eur. J. Enterp. Technol*., 2021, **2**, no. 6, 6–20. doi: 10.15587/1729-4061.2021.224435
27. R. Farahati, S.M.M. Khoshdel, A. Ghaffarinejad and H. Behzadi, Experimental and computational study of penicillamine drug and cysteine as water-soluble green corrosion inhibitors of mild steel, *Prog. Org. Coat*., 2020, **142**, 105567. doi: 10.1016/j.porgcoat.2020.105567
28. L.S. Barreto, T.F. de Almeida, A. de M. Santos, M.S. Tokumoto, F. Cotting and V.R. Capelossi, Evaluation of vegetables residues as corrosion inhibitors, *Research, Society and Development*, 2021, **10**, e28710817409. doi: 10.33448/rsd-v10i8.17409

29. E. Ituen, A. James, O. Akaranta and S. Sun, Eco-friendly corrosion inhibitor from Pennisetum purpureum biomass and synergistic intensifiers for mild steel, *Chin. J. Chem. Eng*., 2016, **24**, 1442–1447. doi: 10.1016/j.cjche.2016.04.028
30. O.Yu. Grafov and L.P. Kazansky, Review on porphyrins, phthalocyanines and their derivatives as corrosion inhibitors, *Int. J. Corros. Scale Inhib*., 2020, **9**, 812–829. doi: 10.17675/2305-6894-2020-9-3-2
31. Yu.I. Kuznetsov, Triazoles as a class of multifunctional corrosion inhibitors. Review. Part II. 1,2,3-Benzotriazole and its derivatives. Iron and steels, *Int. J. Corros. Scale Inhib*., 2020, **9**, 780–811. doi: 10.17675/2305-6894-2020-9-3-1
32. M. Pramudita, S. Sukirno and M. Nasikin, Synergistic corrosion inhibition effect of rice husk extract and KI for mild steel in H_2SO_4 solution, *Bull. Chem. React. Eng. Catal*., 2019, **14**, 697–704. doi: 10.9767/bcrec.14.3.4249.697-704
33. G.K. Shamnamol, J.M. Jacob, R.P and A. Raj, Synergistic effect of salts on the corrosion inhibitive action of plant extract: a review, *J. Adhes. Sci. Technol*., 2021, **35**, 133–163. doi: 10.1080/01694243.2020.1797336
34. T. Peme, L.O. Olasunkanmi, I. Bahadur, A.S. Adekunle, M.M. Kabanda and E. Ebenso, Adsorption and Corrosion Inhibition Studies of Some Selected Dyes as Corrosion Inhibitors for Mild Steel in Acidic Medium: Gravimetric, Electrochemical, Quantum Chemical Studies and Synergistic Effect with Iodide Ions, *Molecules*, 2015, **20**, 16004–16029. doi: 10.3390/molecules200916004
35. R. García-Mata, M.F. Gonzalez-Machorro, R.C. Garcia-Sánchez, J.S. Mora-Flores, A. Gonzales-Estrada and A. Martinez-Damian, Banana (*Musa paradisiaca*) market in Mexico, 1971–2017, *Agrociencia*, 2013, **47**, 399–410. doi: v47n4a8.pdf (scielo.org.mx)
36. G. Blasco López, F.J. Gómez Montaño and V.E. Bolado Garcia, Compositional and antioxidant analysis of peels from different banana varieties (Musa spp.) for their possible use in developing enriched flours, *Med. J. Univ. of Veracruzana*, 2014, **29**, no. 1, 1–14. doi: 10.15174/au.2019.2260
37. H. Li, S. Zhang, and Y. Qiang, Corrosion retardation effect of a green cauliflower extract on copper in H_2SO_4 solution: Electrochemical and theoretical explorations, *J. Mol. Liq*., 2021, **321**, 114450. doi: 10.1016/j.molliq.2020.114450
38. O.O. Ogunleye A.O. Arinkoola, O.A. Eletta, O.O. Agbede, Y.A. Osho, A.F. Morakinyo and J.O. Hamed, Green corrosion inhibition and adsorption characteristics of luffa cylindrica leaf extract on mild steel in hydrochloric acid environment, *Heliyon*, 2020, **6**, e03205. doi: 10.1016/j.heliyon.2020.e03205
39. R. Zhao, Q. Yu, and L. Niu, Corrosion inhibition of amino acids for 316L stainless steel and synergistic effect of I^- ions: Experimental and theoretical studies, *Mater. Corros*., 2022, **73**, 31–44. doi: 10.1002/maco.202112511
40. M. Djellab, H. Bentrah, A. Chala and H. Taoui, Synergistic effect of halide ions and gum arabic for the corrosion inhibition of API5L X70 pipeline steel in H_2SO_4, *Mater. Corros*., 2019, **70**, 149–160. doi: 10.1002/maco.201810203

41. S. Cherrad, I. Jaouadi, Y. El Aoufir, M. Tiskar, B. Satrani, M. Ghanmi, A. Guenbour and A. Chaouch, Unveiling corrosion inhibition properties of the cupressus arizonica leaves essential oil for carbon steel in 1.0 m HCl, *Int. J. Corros. Scale Inhib*., 2020, **9**, no. 2, 607–622. doi: 10.17675/2305-6894-2020-9-2-15
42. I. Dhouibi, F. Masmoudi, M. Bouaziz, and M. Masmoudi, A study of the anti-corrosive effects of essential oils of rosemary and myrtle for copper corrosion in chloride media, *Arabian J. Chem*., 2021, **14**, 102961. doi: 10.1016/j.arabjc.2020.102961
43. Ya.G. Avdeev, L.V. Frolava, D.S. Kuznetsov, M.V. Tyurina and M.A. Chekulaev, Protection of stainless steel in sulfuric acid solution containing hydrogen sulfide by inhibitors, *Int. J. Corros. Scale Inhib*., 2016, **5**, no. 2, 147–158. doi: 10.17675/2305-6894-2026-5-2-4
44. M. Djellab, H. Bentrah, A. Chala, H. Taoui, S. Kherief and B. Bouamra, Synergistic effect of iodide ions and bark resin of Schinus molle for the corrosion inhibition of API5L X70 pipeline steel in H_2SO_4, *Mater. Corros*., 2020, **71**, 1276–1288. doi: 10.1002/maco.202011533
45. M.R. Adam, A.A. Rahim, and A.M. Shah, Synergy between iodide ions and mangrove tannins as inhibitors of mild steel corrosion, *Ann. For. Sci*., 2015, **72**, 9–15. doi: 10.1007/s13595-014-0398-9
46. M. Jokar, T.S. Farahani and B. Ramezanzadeh, Electrochemical and surface characterizations of morus alba pendula leaves extract (MAPLE) as a green corrosion inhibitor for steel in 1 M HCl, *J. Taiwan Inst. Chem. Eng*., 2016, **63**, 436–452. doi: 10.1016/j.jtice.2016.02.027
47. L. Kaghazchi, R. Naderi and B. Ramezanzadeh, Synergistic mild steel corrosion mitigation in sodium chloride-containing solution utilizing various mixtures of phytic acid molecules and Zn^{2+} ions, *J. Mol. Liq*., 2021, **323**, 114589. doi: 10.1016/j.molliq.2020.114589
48. L. Koursaoui, Y. Kerroum, M. Tabyaoui, A. Guenbour A. Bellaouchou, B. Satrani, M. Ghanmi, I. Warad and A. Chaouch, Chemical composition and inhibition effect of eucalyptus botryoides on the corrosion of C38 steel in hydrochloric acid solution, *Biointerface Res. Appl. Chem*., 2021, **11**, 10119–10130. doi: 10.33263/BRIAC113.1011910130
49. B. lan Lin, J. jie Shao, Y. ye Xu, Y. ming Lai, and Z. ning Zhao, Adsorption and corrosion of renewable inhibitor of Pomelo peel extract for mild steel in phosphoric acid solution, *Arabian J. Chem*., 2021, **14**, 103114. doi: 10.1016/j.arabjc.2021.103114
50. P. Manantapong, N. Chaipunya, S. Wannapaiboon, P. Chirawatkul, W. Wattanathana and Y. Hanlumyuang, Efficiency of organic corrosion inhibitors derived from Thai-bael fruit extract for preventing corrosion in carbon steels, *Arabian J. Chem*., 2020, **32**, 2043–2050. doi: 10.14233/ajchem.2020.22743
51. R. Haldhar, D. Prasad and N. Bhardwaj, Surface adsorption and corrosion resistance performance of acacia concinna pod extract: an efficient inhibitor for Mild steel in acidic environment, *Arab. J. Sci. Eng*., 2020, **45**, 131–141. doi: 10.1007/s13369-019-04270-2

52. E.B. Policarpi and A. Spinelli, Application of Hymenaea stigonocarpa fruit shell extract as eco-friendly corrosion inhibitor for steel in sulfuric acid, *J. Taiwan Inst. Chem. Eng*., 2020, **116**, 215–222. doi: 10.1016/j.jtice.2020.10.024
53. Unnimaya, P. Shetty, P. Kumari, and S. Kagatikar, Glutathione as green corrosion inhibitor for 6061Al-SiC(p) composite in HCl medium: electrochemical and theoretical investigation, *J. Solid State Electrochem*., 2023, **27**, 255–270. doi: 10.1007/s10008-022-05315-7
54. S. Jayakumar, T. Nandakumar, M. Vadivel, C. Thinaharan, R.P. George and J. Philip, Corrosion inhibition of mild steel in 1 M HCl using Tamarindus indica extract: electrochemical, surface and spectroscopic studies, *J. Adhes. Sci. Technol*., 2020, **34**, 713–743. doi: 10.1080/01694243.2019.1681156
55. D.G. Ladha, N.K. Ghelichkhah, I.B. Obot, F. Khorrami, J.-Z. Yao and D.D. Macdonald, Experimental and computational evaluation of illicium verum as a novel eco-friendly corrosion inhibitor for aluminium, *Mater. Corros*., 2018, **69**, 125–139. doi: 10.1002/maco.201709581
56. C.M. Fernandes, T.S. Ferreira, N.E. Santos, T.S. Rocha, R. Garrett, R.M. Borges, G. Muricy, A.L. Valverde and E.A. Ponzio, Ircinia strobilina crude extract as corrosion inhibitor for mild steel in acid medium, *Electrochim. Acta*, 2019, **312**, 137–148. doi: 10.1016/j.electacta.2019.04.148
57. S. Al-Baghdadi, T.S. Gaaz, A. Al-Adili, A.A. Al-Amiery and M.S. Takriff, Experimental studies on corrosion inhibition performance of acetylthiophene thiosemicarbazone for mild steel in HCl complemented with DFT investigation, *Int. J. Low-Carbon Technol*., 2021, **16**, 181–188. doi: 10.1093/ijlct/ctaa050
58. S. Nikpour, M. Ramezanzadeh, G. Bahlakeh, B. Ramezanzadeh, and M. Mahdavian, *Eriobotrya japonica Lindl* leaves extract application for effective corrosion mitigation of mild steel in HCl solution: Experimental and computational studies, *Constr. Build. Mater*., 2019, **220**, 161–176. doi: 10.1016/j.conbuildmat.2019.06.005
59. N.R. Devi, N. Karthiga, R. Keerthana, T. Umasankareswari, A. Krishnaveni, G. Singh and S. Rajendran, Extracts of leaves as corrosion inhibitors – An overview and corrosion inhibition by an aqueous extract of henna leaves (Lawsonia inermis), *Int. J. Corros. Scale Inhib*., 2020, **9**, no. 4, 1169–1193. doi: 10.17675/2305-6894-2020-9-4-2
60. M. Pavlidou, M. Pagitsas and D. Sazou, Potential oscillations induced by the local breakdown of passive iron in sulfuric acid media. An evaluation of the inhibiting effect of nitrates on iron corrosion, *J. Solid State Electrochem*., 2015, **19**, 3207–3217. doi: 10.1007/s10008-015-2812-0
61. H.M. Sabaa, K.M. El-Khatib, M.Y. El-Kady and S.A. Mahmoud, Spinel structure of activated carbon supported MFe_2O_4 composites as an economic and efficient electrocatalyst for oxygen reduction reaction in neutral media, *J. Solid State Electrochem*., 2022, **26**, 2749–2763. doi: 10.1007/s10008-022-05269-w

♦ ♦ ♦